Brain Tumour Segmentation using Few-shot Learning

Somashekhar Kinagi [1*†], Akshata Joshi [1†], Bindu Nagashetti [1†], Anjali Savalkar [1†], Bipan Kumar [1†], Dr. Uday Kulkarni [2]

[1]School of Computer Science and Engineering, KLE Technological University, Vidyanagar, Hubballi, 580031, Karnataka, India.

*Corresponding author(s). E-mail(s): 01fe22bcs063@kletech.ac.in;
Contributing authors: 01fe22bcs190@kletech.ac.in;
01fe22bcs291@kletech.ac.in; 01fe22bcs196@kletech.ac.in;
01fe22bcs044@kletech.ac.in; uday_kulkarni@kletech.ac.in;
†These authors contributed equally to this work.

Abstract

Brain tumor segmentation is critical in medical imaging but remains a challenging task due to the limited availability of annotated data. While Deep Neural Networks (DNNs) have demonstrated promising results, they typically require extensive datasets and often struggle to generalize across unseen tumor types. To address these challenges, we propose a novel few-shot learning framework for brain tumor segmentation in Magnetic Resonance Imaging (MRI) using prototype similarity scores. Unlike conventional methods that process entire image sets, our approach focuses on specific slices containing tumor regions, significantly reducing training data requirements. The model employs an iterative training strategy, selecting random tumor slices and pairing them with other slices from the same scan to form a support set. By utilizing metric learning with non-parametric thresholds, the model effectively distinguishes query images from class prototypes. Evaluation on the BraTS 2021 dataset, comprising 360 training and 100 testing MRI scans, highlights the framework's efficiency. The model achieves an F1 Score of 78.96% and a Mean Intersection over Union (mIoU) of 80.97% in a 5-shot 2-way configuration. In a 10-shot 2-way setup, the performance improves, reaching an F1 Score of 81.75% and an mIoU of 81.59%, demonstrating its ability to segment tumor regions more accurately with additional data. These results emphasize the effectiveness of the proposed few-shot learning framework for accurate and efficient brain tumor segmentation in settings with limited data.

Keywords: Few-shot learning, brain tumor segmentation, meta-learning, U-Net architecture, Masked Average Pooling.

1 Introduction

Brain tumors are abnormal growths of cells in the brain, which can range from non-cancerous (benign) to cancerous (malignant). They can disrupt vital brain functions and pose serious health risks. Detecting and segmenting these tumors early is crucial for planning treatments like surgery or radiotherapy. Brain tumors present a significant health burden worldwide. In India, the prevalence is estimated at 5 to 10 cases per 100,000 people, with rising incidence rates [1]. MRI is a highly effective tool for diagnosing brain tumors, offering detailed images of the brain in various modalities that aid in detecting abnormalities. Segmentation is crucial in accurately outlining the tumor boundaries, enabling precise identification and analysis. This process not only ensures accurate identification of the tumor but also distinguishes it from surrounding healthy tissues, edema, and necrotic regions [2].

Manual segmentation by radiologists is the traditional approach to tumor analysis. However, it has drawbacks such as its time-consuming nature. The process can take hours or even days for large datasets. Different experts might draw tumor boundaries differently because of unclear edges or their level of experience. These differences affect treatment decisions, like how much of the tumor to remove or where to focus radiation, potentially impacting the patient's recovery. Automated methods help avoid these problems by providing consistent and accurate results [3]. To address these challenges, deep learning, particularly Convolutional Neural Networks (CNNs), has revolutionized medical image segmentation [4]. CNNs have transformed tumor segmentation by learning patterns directly from data, making them more accurate and reliable than traditional methods.However, despite their advancements, these deep learning techniques often depend on large datasets and powerful computing resources, which can be challenging to access in real-world settings. Additionally, handling variations in tumor appearance and class imbalances remains a persistent issue [5] .

Work focuses on using the Brain Tumor Segmentation (BraTS) dataset with the U-Net model, a well-established architecture in medical image segmentation [6].The BraTS 2021 dataset is a widely used benchmark for brain tumor segmentation, providing multi-parametric MRI scans that capture the diverse characteristics of gliomas. Each sample includes four MRI modalities—Flair, T2, T1ce, and T1—along with ground truth labels. Flair is effective for detecting edema, T2 highlights fluid-filled regions, T1ce focuses on contrast-enhanced tumor areas, and T1 provides detailed anatomical structures. This multimodal approach ensures comprehensive tumor characterization. The dataset encompasses a wide range of tumor sizes, irregular shapes, and both high-grade and low-grade gliomas, reflecting real-world clinical diversity. It also includes detailed annotations of tumor substructures, such as the enhancing tumor, tumor core, and edema, enabling precise segmentation. Furthermore, BraTS 2021 incorporates scans from patients with varying demographics, ensuring the dataset's representativeness. Detecting cancerous tumors early can save lives, but

identifying brain tumors is particularly challenging due to the lack of labeled data for training models. To combine the U-Net model with few-shot learning to improve tumor detection with minimal labeled data [7]. Ensure the model performs well on unseen data, reliably labeling brain tumors with high mIoU (Mean Intersection over Union) [8]. Reduce the dependency on large, annotated datasets, enabling faster and more efficient deployment in clinical settings.In this study, we achieved high accuracy in brain tumor segmentation with minimal labeled data, showing an Average Dice coefficient of 78.42% and Precision of 61.03% in 5-shot scenarios, which improved to 80.89% and 79.62%, respectively, in 10-shot settings. These results underscore its potential for real-world clinical applications. Our method adopts a U-Net as feature extractor. We evaluate segmentation accuracy using Intersection over Union (IoU) metrics [9].

The proposed study is structured into six main sections. Section 2 provides a concise review of the literature on traditional and deep learning methods, highlighting the promise of few-shot learning. Section 3 discusses the proposed methodology, including preprocessing steps, feature extraction, and model architecture. Specifically, it details how MRI slices are processed to focus on relevant regions and explains how VGG-16 and U-Net work together with Masked Average Pooling (MAP) for tumor segmentation. Section 4 presents the results, evaluating the effectiveness of the proposed approach. Section 5 offers conclusions and highlights the study's contributions to future work.

2 Background

Recent advancements in brain tumor segmentation from MRI scans have transitioned from traditional image processing methods to more sophisticated deep learning approaches. Early techniques, such as thresholding, edge detection, and clustering (e.g., K-means), were computationally light but struggled to accurately delineate complex tumor shapes and differentiate them from surrounding tissues. As the field progressed, classical machine learning models like Support Vector Machines (SVM) and Random Forests gained traction, utilizing handcrafted features such as texture and intensity. However, these models were limited by their reliance on manual feature extraction and faced challenges when working with large, complex datasets or subtle tumor variations [10]. The introduction of deep learning, particularly CNNs, marked a significant breakthrough in this area. Models like U-Net enabled pixel-wise predictions with high accuracy, even on smaller datasets, due to their encoder-decoder architecture, that captures both low-level and high-level features [11]. Innovations such as Mask R-CNN and Dense U-Net further enhanced segmentation by incorporating instance-level techniques. Despite these advancements, a persistent challenge remains: acquiring large, annotated datasets for effective training [12]. To tackle the issue of data scarcity, few-shot learning techniques have emerged as a promising solution to achieve efficient segmentation with minimal annotation. Approaches like Prototypical Networks allow models to learn generalized features from only a few labeled examples, demonstrating strong performance on unseen data [13]. This method not only reduces the dependency on extensive annotated datasets but also enhances the model's adaptability to new tumor types. By focusing on the similarity between support and

query images, few-shot learning models can generalize effectively even with limited data. Moreover, few-shot learning is more computationally efficient, making it particularly valuable, especially in medical imaging applications where resources are often constrained [14]. This combination of few-shot learning with deep learning models suggests a promising direction for achieving more accurate and efficient brain tumor segmentation, especially in scenarios where annotated data is scarce or imbalanced [15].

3 Proposed methodology

The proposed work introduces a novel few-shot semantic segmentation approach for brain tumor detection in MRI scans. It leverages MAP to generate prototypes from support images. These prototypes are then used to segment query images, including those from previously unseen tumor classes. The key steps in our approach involve the generation of foreground prototypes by applying MAP to the feature maps of the support images, with the tumor regions highlighted by the binary mask. These prototypes are then aligned with the features of the query image using a convolutional operation, enabling accurate segmentation. We use a U-Net-based decoder to process the aligned query features and create the final segmentation mask. To train the model, we rely on Binary Cross-Entropy (BCE) loss, which helps measure how far the predicted mask is from the actual ground truth. One of the main strengths of the model is its ability to segment new, novel tumor categories. This is made possible by learning the similarities between the support and query images, even when there's only a small amount of labeled data available[16]. During inference, prototypes for new classes are generated from the support images, and these prototypes guide the segmentation of query images from the same class. This framework ensures that the model can effectively generalize to previously unseen tumor types, making it a powerful tool for medical image segmentation in real-world applications [17].

3.1 Preprocessing and feature extraction

In this study, we focused on tumor segmentation in 3D MRI volumes by slicing the data to concentrate on the most relevant sections. MRI volumes consist of multiple 2D slices arranged along the Z-axis. We utilized tools like SimpleITK and Nibabel to load the data stored in NIfTI format, ensuring accurate representation of voxel size and orientation [18]. To standardize the dataset, we resampled the volumes to a uniform voxel spacing of 1x1x1 mm^3. After analysis, we identified that slices between 60 and 135 along the Z-axis were most informative for detecting brain tumors, discarding those outside this range and filtering out slices dominated by background noise.

Once we selected the relevant slices, we prepared them for model input by normalizing pixel intensities to a standard range (e.g., 0–1) and resizing the images to a fixed resolution of 256x256 pixels. Fig 1 illustrates a sample of brain MRI slices after preprocessing and augmentation. Preprocessing steps, such as normalization and noise reduction, ensured data consistency, while augmentation techniques like rotation, flipping, and contrast adjustments increased the diversity of the dataset, improving the model's robustness.

This approach allowed us to focus on critical regions of the MRI volumes, ensuring our dataset was compact and highly relevant for training the tumor segmentation model. By eliminating redundant slices, we improved both the quality and efficiency of the data used for this task [19].

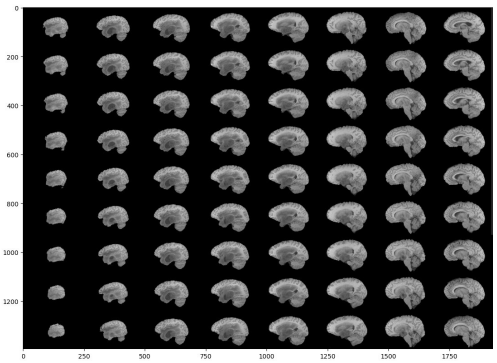

Fig. 1: Visualization of Brain MRI Slices shows after preprocessing (resizing, normalization) and augmentation (rotation, flipping, contrast changes).

3.2 Segmentation model architecture

It consists of two main components: the encoder-decoder architecture for feature extraction and segmentation guidance, and the use of MAP for prototype generation. The following sections provide a detailed explanation of the architecture, highlighting the roles of the VGG-16 encoder and the U-Net decoder. Encoder: The encoder used in the proposed architecture is VGG-16, a CNN pre-trained on ImageNet. VGG-16 is a deep architecture with 16 layers, primarily composed of convolutional layers followed by max-pooling layers [20]. In the context of this framework, VGG-16 is used to extract feature embeddings from both the support and query images, which are critical for tumor segmentation.

In this framework, VGG-16 is effective due to its ability to capture hierarchical features in images. The encoder processes both the support and query images, producing feature embeddings $\mathbf{f}_s \in \mathbb{R}^{H' \times W' \times D}$ for the support image and $\mathbf{f}_q \in \mathbb{R}^{H' \times W' \times D}$ for the query image, where H' and W' denote the spatial dimensions of the feature maps, and D represents the depth (embedding dimension). These embeddings contain rich information about the spatial structure and semantic features in the images, which are essential for distinguishing foreground tumor regions[21].

The Fig. 2 illustrates a few-shot learning framework for segmenting brain tumors in MRI scans. The process starts with T2-weighted MRI slices, which are preprocessed and divided into support and query image-label pairs. The support and query image pairs are input into an Encoder CNN to extract features from both. The features extracted from the support images are then used to generate support prototypes, which serve as representative embeddings of the tumor regions [22].The query features are

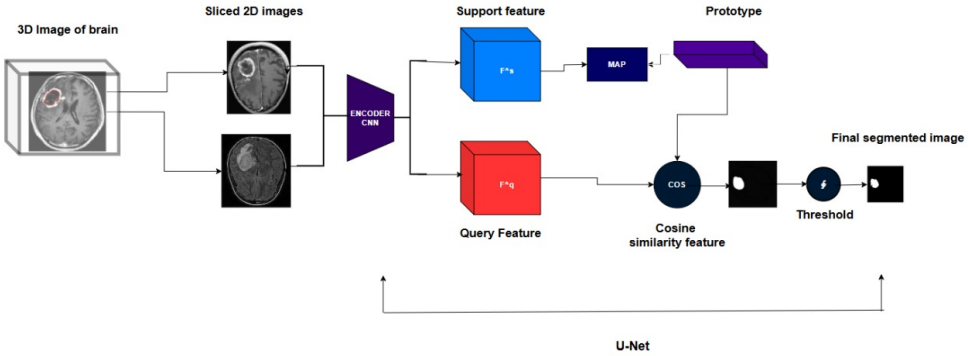

Fig. 2: Prototypical Few-Shot Brain Tumor Segmentation which converts 3D MRI volumes to 2D slices, uses VGG-16 for feature extraction from support and query images, and performs tumor segmentation with few-shot learning.

then compared to the support prototypes using a cosine similarity function, generating a similarity map. This map produces an initial segmentation prediction. To refine the output, a score thresholding step is applied, where predictions are filtered based on a confidence threshold (σ). This refinement step results in the final segmentation mask for the query image. This framework effectively segments tumors even when only a few labeled examples are available. By focusing on the similarities between the support and query images, the model can generalize to new, unseen tumor types. This makes the approach particularly valuable in medical imaging, where obtaining large amounts of annotated data is challenging.

3.3 Masked Average Pooling

Once the feature embeddings are obtained, the next step is to focus on the relevant tumor regions in the support image. This is achieved using MAP, an operation that calculates prototypes for each foreground class by considering only the foreground pixels in the support mask. The support mask $\tilde{Y}_s$ is a binary mask that highlights the tumor region (foreground) and the background [23]. The prototype for each foreground class is computed by averaging the feature embeddings within the regions corresponding to the foreground in the support image, as described by the following equation:

$$p_k = \frac{\sum_{x,y=1}^{W' \times H'} f_s^{(k)}(x,y) \cdot \tilde{Y}_s(x,y)}{\sum_{x,y=1}^{W' \times H'} \tilde{Y}_s(x,y)} \tag{1}$$

Here, p_k represents the k-th prototype, and $f_s^{(k)}(x,y)$ is the k-th feature map from the support image in equation 1. The Hadamard product $\tilde{Y}_s(x,y)$ ensures that only the foreground pixels (where $\tilde{Y}_s(x,y) = 1$) contribute to the average calculation.

3.4 Prototype Expansion and Convolutional Guidance

Once the prototypes are computed, they are aligned with the query feature maps to facilitate segmentation. To achieve this, the prototypes are expanded to match the spatial resolution of the query feature maps using an unpooling operation. This process restores the spatial dimensions of the prototypes, enabling direct comparison with the query feature maps. Instead of relying on traditional similarity measures, the model employs convolution to align the upsampled prototypes with the query feature maps [24]. This convolution acts as a form of guidance, directing attention to the specific regions of the query image associated with the tumor. The convolution operation is mathematically expressed as:

$$f_{\text{guided}} = \text{Conv}(f_q, p_k) \tag{2}$$

Here, f_q represents the query feature map, p_k is the upsampled prototype, and f_{guided} is the resulting guided feature map that emphasizes the object regions in the query image.

3.5 Decoder: U-Net for Segmentation

The decoder in the architecture is inspired by the U-Net framework, a well-known design for image segmentation. U-Net employs an encoder-decoder structure with skip links connecting matching layers of the encoder and decoder [25]. These connections help preserve detailed spatial information from the input image during the down-sampling and up-sampling processes. In this framework, the U-Net decoder processes the *guided feature map* (f_{guided}), which combines query features and prototype information. The decoder progressively refines this feature map to produce a *binary segmentation mask* ($\hat{Y}_q$) for the query image. This mask highlights tumor regions, where pixel values of 1 denote presence and 0 indicate the background. The U-Net decoder consists of several convolutional layers followed by up-sampling layers. As the feature maps are passed through these layers, the model progressively reconstructs the segmentation mask, which is refined by the guidance from the prototypes. The final output is a segmentation mask that accurately delineates the tumor region in the query image.

3.6 Segmentation Loss and Prototype Alignment Regularization

To train the model, the binary cross-entropy loss function is used to minimize the difference between the predicted segmentation mask and the ground truth mask L_{seg} (see Equation (3)). The segmentation loss function is defined as:

$$L_{\text{seg}} = -\sum_{i,j} [\eta(i,j) = c] \log(M_q(i,j)) \tag{3}$$

where $M_q(i,j)$ represents the predicted foreground probability for pixel (i,j) in the query image, and $\eta(i,j)$ denotes the ground truth label for pixel (i,j), which is either background or object.

In addition to the segmentation loss, a prototype alignment regularization loss L_{PAR} is applied to further improve the alignment between the query and support images. This regularization loss encourages the model to minimize the discrepancy between the feature embeddings of the query and support images, ensuring better prototype alignment.

Algorithm 1 Training Few-Shot Segmentation Model with step size β, utilizing episodic learning

Require: Support set $S = \{(x_i^s, y_i^s)\}_{i=1}^{N_s}$, Query set $Q = \{(x_j^q, y_j^q)\}_{j=1}^{N_q}$, and step size β.

for each epoch in training steps **do**
  for each episode (support-query pair) **do**
    Randomly sample K images and corresponding labels to form the support set S.
    Randomly sample query images Q from the dataset that do not overlap with S.
    $f^s \leftarrow f_\theta(x^s)$ ▷ Extract support features
    $f^q \leftarrow f_\theta(x^q)$ ▷ Extract query features using the feature encoder model
    $P_k \leftarrow \rho(f_k^s, y_k^s)$, $\forall k \in \{1, \ldots, K\}$
    Compare f^q with prototypes P_k to generate similarity maps for segmentation.
    $\mathcal{L}_{\text{seg}} \leftarrow \text{CrossEntropy}(f^q, y^q)$
    $\mathcal{L}_{\text{aux}} \leftarrow \text{PrototypeAlignmentLoss}(P_k)$
    $\mathcal{L}_{\text{total}} \leftarrow \mathcal{L}_{\text{seg}} + \mathcal{L}_{\text{aux}}$
    $\theta \leftarrow \theta - \beta \frac{\partial \mathcal{L}_{\text{total}}}{\partial \theta}$ ▷ Update model parameters
  end for
end for

This loss helps improve the flow of information between the support and query feature maps during training, which is crucial for the success of few-shot segmentation tasks [26]. This method employs a pre-trained feature encoder f_θ to extract high-dimensional features from both the support set S and the query set Q. The features from the support set are represented as $x_s = f_\theta(S)$, while the query features are $x_q = f_\theta(Q)$. Using MAP, foreground prototypes P are generated from the support features. The formula for prototype generation is given in Equation (4)

$$P[k] = \rho(x_s^k) \tag{4}$$

where k iterates over all support features, and ρ represents the MAP function, ensuring that only the labeled regions in the support set contribute to the prototype representation. These prototypes encapsulate class-specific characteristics of the regions of interest [27]. To guide the segmentation of query images, the query features x_q are compared to the prototypes P using the cosine similarity function $R(x, y)$, which measures the similarity between two feature vectors x and y. The segmentation predictions are further refined using a thresholding function σ to remove small artifacts

and focus on clinically significant regions. The refined segmentation map highlights the ROIs, such as brain tumors.

Loss functions, including pixel-wise cross-entropy loss and Prototype Alignment Loss (PAR), are employed to optimize the alignment between the support prototypes and the query features, improving segmentation accuracy and robustness [28]. This approach uses episodic training to simulate few-shot scenarios, enabling the model to generalize effectively with minimal labeled data. By combining a robust feature encoder, MAP, and similarity-based segmentation, this method addresses the critical challenge of segmenting medical images with high precision and reliability, making it particularly useful for tasks such as brain tumor detection. The segmentation of query images is guided by a similarity comparison between their feature maps and the computed prototypes [29]. These comparisons generate similarity scores that are transformed into segmentation maps, delineating ROIs in the query images. A combination of loss functions, including pixel-wise cross-entropy loss and auxiliary terms such as PAR, ensures effective optimization of the model [30]. These losses refine the alignment between support prototypes and query features, enhancing segmentation accuracy and robustness.

The proposed method adopts an episodic framework to train the model, as outlined in **algorithm 1**, which aligns with the few-shot learning paradigm. The model's training process involves exposure to diverse segmentation tasks, enabling it to generalize effectively to unseen classes and datasets. It isolates class-relevant features and suppresses background noise, allowing prototypes to encapsulate meaningful semantic information. Auxiliary loss functions like Prototype Alignment Loss improve the model's robustness in handling complex medical imaging tasks.

4 Results

The results of our few-shot semantic segmentation model, trained on the BraTS 2021 dataset with 360 training images and 100 testing images, offer significant insights into its performance.

Table 1: Score Metrics of different models used for brain tumor segmentation

Method	**Avg. Dice%**	**Avg. IoU%**	**Precision%**
Few-shot TL	52.73	65.85	61.81
Few-shot ML	66.98	73.41	64.87
ResUNet	70.20	68.68	63.29
5-shot 2-way	78.42	80.97	76.03
10-shot 2-way	80.89	81.59	79.62

The findings, summarized in Table 1, indicate that increasing the number of samples in the support set provides minimal improvement in performance metrics due to the random selection of slices and the variability in tumor sizes, shapes, and intensities.

This variability negatively impacts the model's ability to segment tumors accurately, as metrics like precision, Dice Score, and IoU reflect challenges in distinguishing tumor from non-tumor regions, capturing consistent boundaries, and generalizing across diverse tumor geometries and intensities as shown in Fig. 3.

Despite the challenges of segmenting brain tumors with limited data, Table 1 demonstrates the effectiveness of the different models. The 5-shot 2-way approach achieves an Average Dice coefficient of 78.42 and a Mean IoU of 80.97%, indicating its ability to predict tumor regions with reasonable overlap and spatial alignment. With a Precision of 76.03%, Recall of 82%, and an F1 Score of 78.96%, it showcases a balanced performance, although the slightly lower Precision suggests some false positives. The 10-shot 2-way approach shows marked improvements, achieving an Average Dice coefficient of 80.89, a Mean IoU of 81.59%, a Precision of 79.62%, a Recall of 84%, and an F1 Score of 81.75%, demonstrating its enhanced ability to segment tumor regions more accurately.

Few-shot learning using prototype learning achieves competitive results compared to traditional methods like fully-supervised deep learning models, which typically require large annotated datasets and achieve higher Dice scores (85-90%) at the cost of extensive labeling efforts. The few-shot prototype learning approach, however, achieves reasonably high Dice and IoU scores with only a small support set, offering a practical trade-off between accuracy and data requirements. ResUNet, while achieving the best baseline Dice, struggles with false positives, reflected in a lower Precision. The 5-shot 2-way and 10-shot 2-way approaches show improvements in segmentation performance as the number of labeled samples increases. The model demonstrates computational efficiency with reduced training time and lower resource usage, further emphasizing its scalability and cost-effectiveness. However, the results section lacks comparisons with contemporary methods, making it difficult to fully validate the claim of superior performance. While the potential of few-shot learning for brain tumor segmentation in data-scarce scenarios is evident, additional quantitative details on training time and resource usage would strengthen the case for its practical applicability in medical imaging tasks.

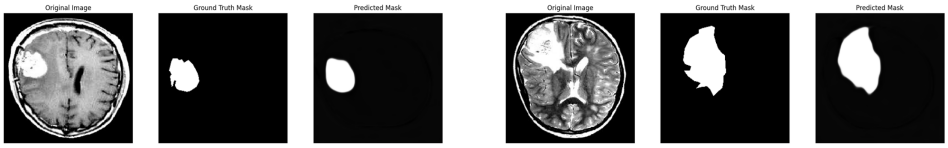

Fig. 3: Illustration of brain tumor segmentation highlighting predicted tumor regions.

5 Conclusion and Future work

The study presents a prototype-based few-shot learning model for brain tumor segmentation in MRI scans, addressing data scarcity, computational complexity, and segmentation accuracy in medical imaging. The model achieved a precision of 79.62%

and a mean IoU of 81.59%, demonstrating its ability to segment tumor regions with minimal labeled data and computational resources. Its efficiency lies in its small number of training images (360 MRI scans), making it suitable for clinical settings where large annotated datasets are often limited. The model's generalizability to unseen tumor types also demonstrates its potential for diverse medical contexts.

The single-prototype approach limits the model's application to multi-class tasks, such as differentiating edema, necrotic regions, and enhancing tumor cores. Effective multi-class segmentation requires generating multiple prototypes to accurately represent distinct classes, which the current model lacks. Addressing these limitations calls for exploring hierarchical or instance-specific prototypes and dynamic prototype generation mechanisms. Incorporating additional contextual features, like spatial or texture information, into the prototype alignment process could further improve segmentation accuracy for irregular shapes. These advancements would enhance the model's robustness and expand its applicability to complex medical imaging tasks and clinical scenarios.

References

[1] Karim, S., Tong, G., Yu, Y., Laghari, A.A., Khan, A.A., Ibrar, M., Mehmood, F.: Developments in brain tumor segmentation using mri: Deep learning insights and future perspectives. IEEE Access (2024)

[2] Abdusalomov, A.B., Mukhiddinov, M., Whangbo, T.K.: Brain tumor detection based on deep learning approaches and magnetic resonance imaging. Cancers **15**(16), 4172 (2023)

[3] García-Figueiras, R., Baleato-González, S., Luna, A., Padhani, A.R., Vilanova, J.C., Carballo-Castro, A.M., Oleaga-Zufiria, L., Vallejo-Casas, J.A., Marhuenda, A., Gómez-Caamaño, A.: How imaging advances are defining the future of precision radiation therapy. RadioGraphics **44**(2), 230152 (2024)

[4] Liu, C., Dong, Y., Xiang, W., Yang, X., Su, H., Zhu, J., Chen, Y., He, Y., Xue, H., Zheng, S.: A comprehensive study on robustness of image classification models: Benchmarking and rethinking. International Journal of Computer Vision, 1–23 (2024)

[5] Xu, Y., Quan, R., Xu, W., Huang, Y., Chen, X., Liu, F.: Advances in medical image segmentation: A comprehensive review of traditional, deep learning and hybrid approaches. Bioengineering **11**(10), 1034 (2024)

[6] Dong, H., Yang, G., Liu, F., Mo, Y., Guo, Y.: Automatic brain tumor detection and segmentation using u-net based fully convolutional networks. In: Medical Image Understanding and Analysis: 21st Annual Conference, MIUA 2017, Edinburgh, UK, July 11–13, 2017, Proceedings 21, pp. 506–517 (2017). Springer

[7] Protonotarios, N.E., Katsamenis, I., Sykiotis, S., Dikaios, N., Kastis, G.A.,

Chatziioannou, S.N., Metaxas, M., Doulamis, N., Doulamis, A.: A few-shot u-net deep learning model for lung cancer lesion segmentation via pet/ct imaging. Biomedical Physics & Engineering Express **8**(2), 025019 (2022)

[8] Vinod, D., Prakash, S.S., AlSalman, H., Muaad, A.Y., Heyat, M.B.B.: Ensemble technique for brain tumour patient survival prediction. IEEE Access (2024)

[9] Albishri, A., Shah, S.J.H., Lee, Y., Wang, R.: Ocu-net: A novel u-net architecture for enhanced oral cancer segmentation. arXiv preprint arXiv:2310.02486 (2023)

[10] Rai, H.M., Yoo, J., Razaque, A.: Comparative analysis of machine learning and deep learning models for improved cancer detection: A comprehensive review of recent advancements in diagnostic techniques. Expert Systems with Applications, 124838 (2024)

[11] Neamah, K., Mohamed, F., Adnan, M.M., Saba, T., Bahaj, S.A., Kadhim, K.A., Khan, A.R.: Brain tumor classification and detection based dl models: A systematic review. IEEE Access (2023)

[12] Salehi, A.W., Khan, S., Gupta, G., Alabduallah, B.I., Almjally, A., Alsolai, H., Siddiqui, T., Mellit, A.: A study of cnn and transfer learning in medical imaging: Advantages, challenges, future scope. Sustainability **15**(7), 5930 (2023)

[13] Liu, Z., Kainth, K., Zhou, A., Deyer, T.W., Fayad, Z.A., Greenspan, H., Mei, X.: A review of self-supervised, generative, and few-shot deep learning methods for data-limited magnetic resonance imaging segmentation. NMR in Biomedicine, 5143 (2024)

[14] Li, M., Jiang, Y., Zhang, Y., Zhu, H.: Medical image analysis using deep learning algorithms. Frontiers in Public Health **11**, 1273253 (2023)

[15] Hussain, D., Al-Masni, M.A., Aslam, M., Sadeghi-Niaraki, A., Hussain, J., Gu, Y.H., Naqvi, R.A.: Revolutionizing tumor detection and classification in multimodality imaging based on deep learning approaches: methods, applications and limitations. Journal of X-Ray Science and Technology (Preprint), 1–55 (2024)

[16] Cao, L., Guo, Y., Yuan, Y., Jin, Q.: Prototype as query for few shot semantic segmentation. Complex & Intelligent Systems **10**(5), 7265–7278 (2024)

[17] Wu, X., Gao, Z., Chen, X., Wang, Y., Qu, S., Li, N.: Support-query prototype fusion network for few-shot medical image segmentation. arXiv preprint arXiv:2405.07516 (2024)

[18] Karami, M.: Machine learning algorithms for radiogenomics: Application to prediction of the mgmt promoter methylation status in mpmri scans. PhD thesis, Politecnico di Torino (2022)

[19] Batool, A., Byun, Y.-C.: Brain tumor detection with integrating traditional and computational intelligence approaches across diverse imaging modalities-challenges and future directions. Computers in Biology and Medicine, 108412 (2024)

[20] Swain, S., Tripathy, A.K.: Automatic detection of potholes using vgg-16 pre-trained network and convolutional neural network. Heliyon **10**(10) (2024)

[21] Liu, C., Amodio, M., Shen, L.L., Gao, F., Avesta, A., Aneja, S., Wang, J.C., Del Priore, L.V., Krishnaswamy, S.: Cuts: A deep learning and topological framework for multigranular unsupervised medical image segmentation. In: International Conference on Medical Image Computing and Computer-Assisted Intervention, pp. 155–165 (2024). Springer

[22] Weng, Y., Zhang, Y., Wang, W., Dening, T.: Semi-supervised information fusion for medical image analysis: Recent progress and future perspectives. Information Fusion, 102263 (2024)

[23] Zhou, L., Zhang, Y., Zhang, J., Qian, X., Gong, C., Sun, K., Ding, Z., Wang, X., Li, Z., Liu, Z., et al.: Prototype learning guided hybrid network for breast tumor segmentation in dce-mri. IEEE Transactions on Medical Imaging (2024)

[24] Tang, P., Li, J., Ding, F., Chen, W., Li, X.: Psnet: Change detection with prototype similarity. The Visual Computer **38**(11), 3541–3550 (2022)

[25] Kazerouni, I.A., Dooly, G., Toal, D.: Ghost-unet: an asymmetric encoder-decoder architecture for semantic segmentation from scratch. IEEE Access **9**, 97457–97465 (2021)

[26] Li, C., Denison, T., Zhu, T.: A survey of few-shot learning for biomedical time series. arXiv preprint arXiv:2405.02485 (2024)

[27] Cheng, G., Lang, C., Han, J.: Holistic prototype activation for few-shot segmentation. IEEE Transactions on Pattern Analysis and Machine Intelligence **45**(4), 4650–4666 (2022)

[28] Li, Q., Sun, B., Xiao, F., Qi, Y., Bhanu, B.: Symmetrical joint learning support-query prototypes for few-shot segmentation. arXiv preprint arXiv:2407.19306 (2024)

[29] Goni, M.R., Ruhaiyem, N.I.R., Mustapha, M., Achuthan, A., Nassir, C.M.N.C.M.: Brain vessel segmentation using deep learning—a review. IEEE Access **10**, 111322–111336 (2022)

[30] Lenczner, G.: Interactive semantic segmentation of aerial images with deep neural networks. PhD thesis, Université Paris-Saclay (2022)